AN ACOUSTIC TECHNIQUE FOR THE MEASUREMENT OF ABSORPTION COEFFICIENTS OF AEROSOL PARTICLES

by

Robert Lee Swinford

A Thesis Submitted to the Faculty of the

DEPARTMENT OF ATMOSPHERIC SCIENCE

In Partial Fulfillment of the Requirements
For the Degree of

MASTER OF SCIENCE

In the Graduate College

THE UNIVERSITY OF ARIZONA

1 9 7 5

STATEMENT BY AUTHOR

This thesis has been submitted in partial fulfillment of requirements for an advanced degree at The University of Arizona and is deposited in the University Library to be made available to borrowers under rules of the Library.

Brief quotations from this thesis are allowable without special permission, provided that accurate acknowledgment of source is made. Requests for permission for extended quotation from or reproduction of this manuscript in whole or in part may be granted by the head of the major department or the Dean of the Graduate College when in his judgment the proposed use of the material is in the interests of scholarship. In all other instances, however, permission must be obtained from the author.

SIGNED: Robert Lee Swinford

APPROVAL BY THESIS DIRECTOR

This thesis has been approved on the date shown below:

R. M. Schotland — 11 August 1975

R. M. Schotland
Professor of Atmospheric Science

Date

TABLE OF CONTENTS

LIST OF ILLUSTRATIONS

ABSTRACT

The "resonant spectrophone" technique may prove to be very useful in the measurement of absorption coefficients of atmospheric aerosols and particulates. The particular choice of a resonant sample chamber deserves detailed consideration.

The mechanism by which modulated light energy absorbed by the particles becomes available as acoustic energy is studied, leading to a constraint placed on the modulation frequency. The theory of the cylindrical resonant sample chamber including energy loss mechanisms and coupling of the optical source is presented for the radial and longitudinal modes. The resulting expressions for the pressure response are examined in terms of their dependence on the geometrical parameters of the chamber.

Experiments are performed on the cylindrical chamber as well as the radial modes of an elliptical chamber. The results indicate that the chamber damping is in only qualitative agreement with the theory. However, the dependence on the geometrical parameters appears to be justified. The final choice of using longitudinal modes is based on a more practical size of chamber and less stringent controls on the stability of the system.

CHAPTER 1

INTRODUCTION

In recent years a great deal of interest has been generated in the use of an opto-acoustic technique for the measurement of concentrations of trace gases. A study by Kruezer (1971) showed that by optically exciting a trace gas specie with a narrow bandwidth source, corresponding to one of the vibrational-rotational absorption bands of the specie, in a cyclic manner a pressure wave is generated; the pressure amplitude being proportional to the trace gas concentration. In further studies Compton (1969) and Kamm (1973) have examined the possibility of coupling the pressure wave into a resonant mode of the sample chamber. The advantage is that the sample chamber acts as an acoustic amplifier to signals at the resonant frequency thus providing an effective gain to such signals.

It is thought that the "resonant spectrophone" technique can be extended and adapted to measure absorption of light energy by atmospheric aerosols and particulates. The amount and distribution of solar energy absorbed by aerosols is an important question in atmospheric science. Aerosol sizes of interest (0.01 - 10.0 microns) do not absorb in bands like gases. A narrow bandwidth optical source is not essential. However, since there is interest in the wavelength dependence of the absorption, the use of a white light source with broad band optical filters should be adequate.

The fraction of energy absorbed by the aerosols per unit length is given by the volume absorption coefficient, α, hereafter referred to simply as the absorption coefficient. An important part of this study is to determine the conditions under which the absorption coefficients can be measured directly. Under most circumstances the absorption coefficients are small ($\sim 10^{-7}-10^{-8} cm^{-1}$); thus the energy absorbed is small. In order to obtain the maximum possible signal under favorable experimental conditions, a proper choice of the resonant sample chamber is necessary. Two geometries chosen for study are the circular cylinder and the elliptical cylinder. The theory of the circular cylinder is presented for radial and longitudinal modes including energy damping mechanisms and optical source coupling. Comparisons based on experiment and theory allow for the optimum choice of the sample chamber, which can then be integrated into a complete "resonant spectrophone" system.

CHAPTER 2

THEORETICAL DISCUSSION

2.1 Description of Energy Transfer from Aerosol Particles

The analysis of the resonant spectrophone technique necessarily begins with an understanding of the absorption of light energy by the particles and the subsequent transfer of this energy to the surrounding medium

Consider a light source having a plane parallel intensity I, modulated at a frequency $f = \frac{\omega}{2\pi}$ so that the intensity satisfies the relation,

$$I = \tfrac{1}{2} I_o \,(1 + \cos\omega t) \tag{2.1}$$

where I_o is the maximum intensity at a point in space. If the volume absorption coefficient at a particular wavelength is α_λ, then the rate of energy absorbed per unit volume, Q, is $\alpha_\lambda I$ where I is assumed to be at the same wavelength λ. Since only the time varying part of I provides useful information, the constant term in (2.1) can be neglected.

$$Q_o = \frac{\alpha_\lambda I_o}{2} \cos\omega t \tag{2.2}$$

This result is valid for small absorption coefficients so that I_o does not effectively change with distance.

It is necessary to determine the extent to which this absorbed energy becomes available in a source of acoustic energy. Therefore we determine the rate of heat transfer from one particle to the medium and then generalize by including a distribution of particles.

Consider a spherical particle of radius a. We introduce the Knudsen number, Kn, defined as the ratio of the molecular mean free path in air, ℓ, to the radius of the particle. In the limit as Kn $\rightarrow$ 0 the heat transfer problem becomes classical. The rate of heat transfer from a spherical particle of radius a for the classical case is given by,

$$Q_c = 4\pi a \chi T' \tag{2.3}$$

Where χ is the thermal conductivity of the medium. If the absolute temperature of the particle is T and the temperature of the medium is T_0 then $T' = T - T_0$. An expression is derived (Fuchs and Sutugin, 1970, p. 64) for the rate of heat transfer in the kinetic transfer case, i.e., for large Kn (Kn is the order of 50 for a = 0.01 microns).

$$Q_k = \pi a^2 \, n_g \, \bar{v}_g \, (c_v + \tfrac{1}{2}k)\alpha_T T' \tag{2.4}$$

n_g is the number density of molecules in the medium; $\bar{v}_g$ is the average velocity of a molecule; c_v is the heat capacity per molecule at constant volume for the medium and k is the Boltzman constant. α_T, the thermal accommodation coefficient, is a measure of whether a molecule colliding with the particle takes on the temperature of the particle ($\alpha_T = 1$) or some fraction of the temperature ($\alpha_T < 1$). The value of

α_T depends on the nature of the particle and is not well known. We will use a value of $\alpha_T = 1$ which may overestimate Q_k in some instances. Fuchs and Sutugin (1970, p. 64) state that the thermal conductivity can be expressed as,

$$\chi = 0.5\ \varepsilon\ c_v\ n_g\ \bar{v}_g\ \ell \tag{2.5}$$

where ε is a dimensionless coefficient whose value is 2.5 for a monatomic gas and 1.9 for a diatomic gas. Making the substitution for $n_g \bar{v}_g$ in (2.4) yields,

$$Q_k = \frac{(c_v + \frac{1}{2}k)\alpha_T}{2\ \varepsilon\ c_v\ K_n}\ 4\pi a \chi T' \tag{2.6}$$

We desire to find a general expression for the rate of heat transfer, Q, applicable at all Knudsen numbers. Sherman's "universal" formula (Fuchs and Sutugin, 1970, p. 65) is an expression for the heat transfer at any Knudsen number, which approaches the classical and kinetic results in the appropriate limits. Fuchs and Sutugin (1970, p. 66) indicate that comparison of Sherman's formula with experimental results of Takao show good agreement. Sherman's formula is,

$$Q = \frac{1}{1 + \frac{\beta\alpha_T}{Kn}}\ Q_k \tag{2.7}$$

where $= \dfrac{c_v + \frac{1}{2}k}{2\ \varepsilon\ c_v}$. It is immediately obvious from (2.7) that for Kn large, $Q \to Q_k$. To show the other limiting case, we substitute into (2.7) the value of Q_k from (2.6) in terms of β, yielding

$$Q = \frac{\frac{\beta\alpha_T}{Kn}}{1 + \frac{\beta\alpha_T}{Kn}} \, 4\pi a\chi T' \tag{2.8}$$

which after rearranging terms yields,

$$Q = \frac{1}{1 + \frac{Kn}{\alpha_T\beta}} \, 4\pi a\chi T. \tag{2.9}$$

The second limiting case is now evident by setting Kn = 0 and comparing with (2.3). The rate of energy transfer per particle can be found from (2.9) once T' is known.

In order to simplify this problem, we assume that the temperature within the particle is spatially isothermal. The rate of heat flow away from the particle is proportional to the thermal conductivity of the medium into which the heat is flowing, i.e., air. For the same particle the rate of heat flow within the particle is proportional to the thermal conductivity of the particle. For almost all materials the thermal conductivity of the particles is much greater than the thermal conductivity of air. Thus as heat is removed by the air with a correspondingly long time constant there is sufficient time for the heat within the particle to flow in such a way as to maintain the spatial uniformity.

The absorption cross section for the particle at a particular wavelength is α_λ. The energy balance requires that the energy absorbed by the particle be either stores in the particle, transferred to the medium by conduction or radiated as black-body energy.

$$\frac{\alpha_\lambda I_o}{2} \cos\omega t = \rho c V \frac{dT'}{dt} + \frac{1}{1 + \frac{Kn}{\alpha_T \beta}} 4\pi a \chi T' + 16\pi\ a^2 \sigma_B T_o{}^3 T' \qquad (2.10)$$

ρ is the density of the particle; c is the specific heat capacity of the particle; V is the volume of the particle, equal to $\frac{4}{3}\pi a^3$ for a sphere. The last term is the upper limit to radiational loss with emissivity = 1, found by taking the black-body function and expanding it in a power series about the ambient temperature T_o, retaining only the first term for T' small. The second and third terms on the right in (2.10) vary linearly with T'. The ratio of the radiative term to the conduction term is $\dfrac{(1 + \frac{Kn}{\alpha_T \beta})\ 4a\sigma_B T_o{}^3}{\chi}$.

Taking $\alpha_T = 1.0$, β from (2.7) is $\frac{6}{19}$ for a diatomic gas, ℓ = 0.5 microns, and room temperature (20^{0}C), for a particle of 10 micron radius the ratio is approximately 0.005 and decreases for smaller particles. Therefore radiational losses can be neglected and (2.10) is simplified.

$$\frac{\alpha_\lambda I_o}{2} \cos\omega t = \rho c V \frac{dT'}{dt} + \frac{1}{\frac{Kn}{\alpha_T \beta}} 4\pi a \chi T' \qquad (2.11)$$

The solution to the homogeneous equation is exponentially damped and approaches zero with a time constant the order of 20 micro-seconds for a 1.0 micron radius particle. The characteristic time is shorter for decreasing particle size. For the inhomogeneous equation a solution is assumed to be of the form,

$$T' = A \cos\omega t = B \sin\omega t \qquad (2.12)$$

Substituting (2.12) into (2.11) yields the solution.

$$T'(t) = \frac{\alpha_\lambda I_o}{2\left[\left(1 + \dfrac{4\pi a\chi}{\dfrac{Kn}{\alpha_T \beta}}\right)^2 + (\rho c V\omega)^2\right]^{\frac{1}{2}}} \cos(\omega t - \delta) \qquad (2.13)$$

$$\text{where} \quad \delta = \mathrm{Tan}^{-1}\left[\frac{\left(1 + \dfrac{Kn}{\alpha_T \beta}\right.(\rho c V\omega)}{4\pi a\chi}\right]$$

The rate of energy transferred from the particles to the air can now be found by substituting (2.13) into (2.9). The result is obtained after rearrangement of terms.

$$Q = \frac{\alpha_\lambda I_o}{2\left[1 + \left(1+\dfrac{Kn}{\alpha_T \beta}\right)^2 \left(\dfrac{\rho c V\omega}{4\pi a\chi}\right)^2\right]^{\frac{1}{2}}} \cos(\omega t - \delta) \qquad (2.14)$$

Equation (2.14) represents the rate of energy transfer per particle to the atmosphere. If the number of particles per unit volume per unit increment of radius is n = n(a) and the limits on the distribution are a_1 and a_2, then the rate of energy transfer to the air per unit volume which represents the source of acoustic energy is

$$W(t) = \int_{a_1}^{a_2} n(a)\ Q(a,t)\ da \tag{2.15}$$

Substituting in for Q(a,t) from (2.14) leads to the result

$$W(t) = \int_{a_1}^{a_2} \frac{n(a)\ \sigma_\lambda(a)\ I_o}{2\left[1 + \left(1+\frac{Kn}{\alpha_T\beta}\right)^2 \left(\frac{\rho c V\omega}{4\pi a \chi}\right)^2\right]^{\frac{1}{2}}} \cos(\omega t - \delta) da \tag{2.16}$$

α_λ is shown to be, Atwater (1971, p. 1368)

$$\alpha_\lambda = \int_{a_1}^{a_2} n(a)\ \sigma_\lambda\ (a)\ da \tag{2.17}$$

If we substitute (2.17) into (2.2) and note that neither I_o nor cos (ωt) depend on a, then the expression for Q_o becomes

$$Q_o\ (t) = \int_{a_1}^{a_2} \frac{n(a)\sigma_\lambda\ (a) I_o}{2} \cos(\omega t)\ da \tag{2.18}$$

In order for all the energy absorbed by the particles during a modulation period to be transferred to the atmosphere within the modulation period, thus becoming available as the acoustic source, it is necessary for (2.16) to equal (2.18) over the appropriate range of particle sizes. This requires the second term in the denominator of (2.16) to be much smaller than 1 which will also allow the phase angle to vanish. The only variable which we command is ω. We assume the thermal accommodation coefficient to be 1.0 as before. For a number of materials the product of ρ and c is very similar and a value of $\rho c = 0.5$ cal cm^{-3} K^{-1} is typical. For a particle of 1.0 micron radius and a modulation frequency of f = 300 Hz approximately 2% of the energy absorbed is returned to the air in a time longer than the modulation period so that it is lost from the acoustic source. The losses approach zero with decreasing particle size.

Under the above constraint placed on the modulation frequency, (2.2) is the acoustic source function indicating that the absorption coefficient can be measured directly. However only a fraction of this energy will contribute to the enhancement of a particular acoustic mode of the sampling chamber. The constraint placed on the modulation frequency noted above will affect the sample chamber geometry for a particular resonant mode. It is necessary, then, to determine how the coupling between the source and the resonant modes is affected by the chamber geometry in order to optimize the system.

2.2 Acoustically Resonant Sample Chamber

The transfer of energy to the medium as discussed in the previous section leads to an increase in the translational energy of the air molecules. This in turn results in a local pressure increase. Since the source is modulated, periodic pressure fluctuations exist which constitute the acoustic signal. Depending on the sample chamber geometry, there are several possibilities for obtaining a resonant situation. For example, for a long tube with a cylindrical cross section radial modes are excited if the source lies along the axis of symmetry. On the other hand if the source lies at one end of the tube longitudinal modes can be excited. Another type of radial mode is obtained with a chamber having an elliptical cross-section. The source lies along one focal line and using the focussing properties of the ellipse, the signal can be measured at the other focal line. These three resonant modes are shown in figure 1.

Prediction of the pressure response of the sample chamber to the modulated source requires the solution of the wave equation with the inclusion of forcing and damping functions which act on the standing wave field. Solution for the elliptical geometry requires the wave equation expressed in elliptical coordinates. The complexity of the solution is beyond the scope of this study so that only radial modes in cylindrical geometry will be theoretically treated. Comparisons of the radial geometry with elliptical will be based on experimental results.

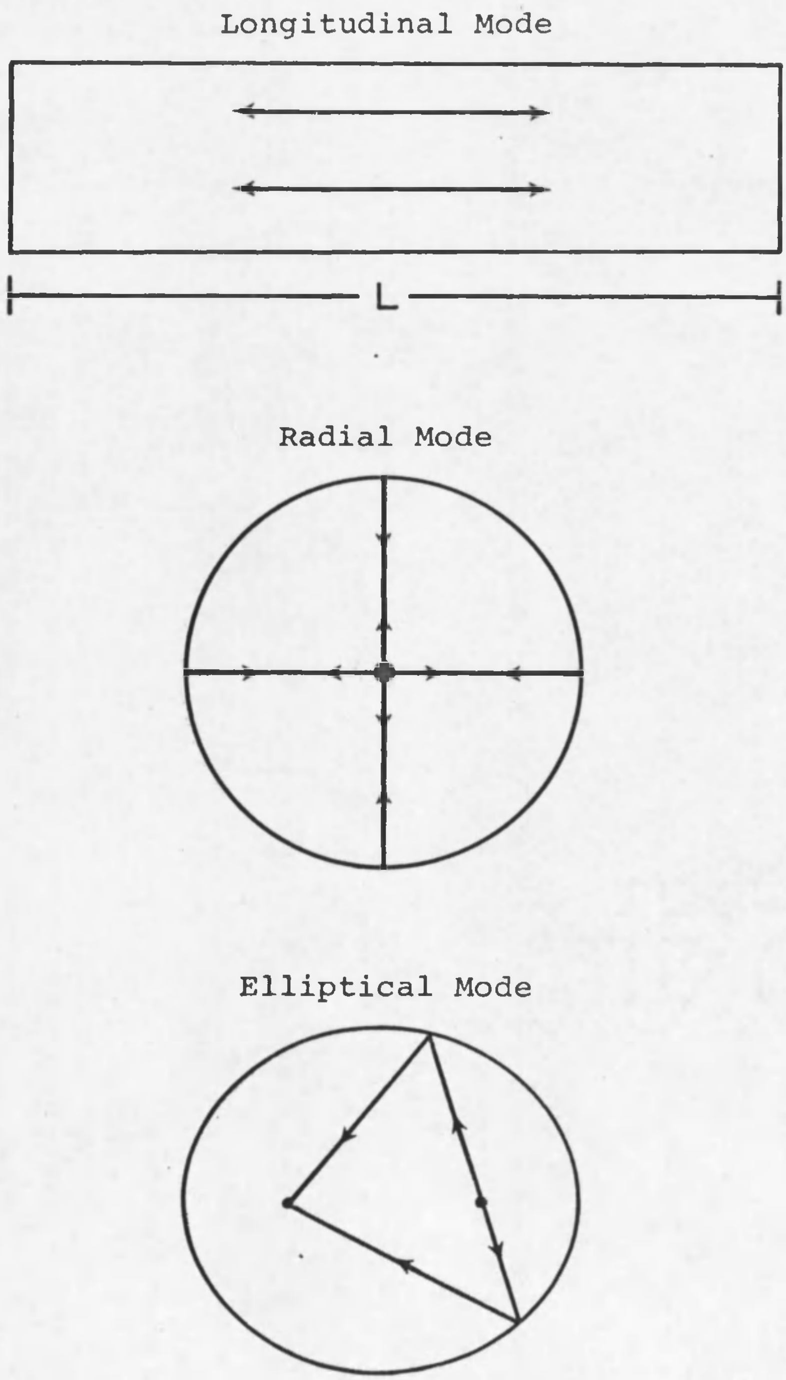

Fig. 1. Resonant Mode Configurations

The description of the cylindrical chamber begins with the governing equations of the systems (Kamm, 1973, p. 18). The fundamental equations are linearized by the perturbation method where primed quantities are perturbations as referenced to the unperturbed state indicated by zeroes.

$$\frac{\partial \rho'}{\partial t} + \rho_o \Delta . \vec{v}' = 0 \quad \left[\frac{\partial \rho'}{\partial t} + \rho_o \Delta u'' = 0 \right] \quad \text{Continuity} \quad (2.19)$$

$$\rho_o \frac{\partial v'}{\partial t} + \nabla \rho' = K_o \vec{v}' \quad \left[\rho_o \frac{\partial u'}{\partial t} + \nabla p' = K_o u' \right] \quad \text{Motion} \quad (2.20)$$

$$\rho \frac{\partial h}{\partial t} - \frac{\partial \rho'}{\partial t} = Q \quad \text{Energy} \quad (2.21)$$

$$P_o = \rho_o R T_o \quad (2.22a)$$

Ideal gas

$$\frac{P'}{P_o} = \frac{\rho'}{\rho_o} + \frac{T'}{T_o} \quad (2.22b)$$

ρ is the density of the medium, V' is the bulk velocity of the molecules, P is the pressure, h is the specific enthalpy, Q is the energy source, R is the specific gas constant and T is the temperature $K_o = \frac{\rho o \omega}{q}$ is a damping factor where it will be shown the q is the quality factor "q" of the resonance. The use of an equivalent body force proportional to the perturbation velocity to account for damping due to interaction of the wave with the chamber walls is indicated by Rayleigh (1945, sections 347-350).

Since the medium behaves as an ideal gas, the enthalpy can be replaced with

$$h = c_p T' \quad (2.23)$$

Using (2.23) with (2.22) results in,

$$\rho_o \frac{\partial h}{\partial t} \quad \frac{\partial p'}{\partial t} = \frac{1}{\gamma-1} + \frac{\partial p'}{\partial t} - \frac{c^2}{\gamma-1} \frac{\partial \rho}{\partial t} \tag{2.24}$$

where $\gamma = \frac{c_p}{c_v}$ and $c^2 = \gamma R T_o$ is the adiabatic speed of sound squared.

A revised energy equation is obtained by substituting the result of (2.24) into (2.21).

$$\frac{\partial p'}{\partial t} - c^2 \frac{\partial \rho'}{\partial t} = (\gamma-1)\ Q \tag{2.25}$$

Following Compton (1969, p. 16) it is convenient to introduce a velocity potential ϕ which defines the perturbation velocity and pressure by $\vec{v}' = \nabla\phi$ (2.26)

$$p' = -K_o\phi + \rho_o \frac{\partial \phi}{\partial t} \tag{2.27}$$

The equation of motion (2.20) is identically satisfied by (2.26) and (2.27).

Substituting (2.26) into (2.19) results in,

$$\frac{\partial \rho'}{\partial t} = -\ \rho_o \nabla^2 \phi \tag{2.28}$$

combining (2.27), (2.28) and (2.25) leads to the desired result.

$$\frac{1}{c^2} \frac{\partial^2 \phi}{\partial t^2} - \nabla^2 \phi + \frac{K_o}{\rho_o c^2} \frac{\partial \phi}{\partial t} = -\left(\frac{\gamma-1}{\rho_o c^2}\right) Q \tag{2.29}$$

This can be recognized as the wave equation with the added damping term $\frac{K_o}{\rho_o c^2} \frac{\partial \phi}{\partial t}$ and the forcing term $-(\frac{\gamma-1}{\rho_o c^2})Q$

Substitution of $K_o = \frac{\rho_o \omega}{q}$ into (2.29) yields.

$$\frac{1}{c} \frac{\partial^2 \Phi}{\partial t^2} - \nabla^2 \phi + \frac{\omega}{qc^2} \frac{\partial \phi}{\partial t} = -(\frac{\gamma-1}{\rho_o c^2})Q \tag{2.30}$$

The boundary conditions on the system are that at the chamber wall normal to the wave direction there is no fluid motion. In terms of the velocity potential ϕ,

$$\begin{aligned} \frac{\partial \phi}{\partial r} &= 0 \quad \text{at } r = R \quad \text{radial modes} \\ \frac{\partial \phi}{\partial z} &= 0 \quad \text{at } z = o, L \quad \text{longitudinal modes} \end{aligned} \tag{2.31}$$

For the first case, purely radial modes will be examined. In the most general case the source function, Q, will be a function of the radial distance, r, as well as time. For a purely modulated source, Q(r,t) may be separated into,

$$Q(r,t) = W(r)\, e^{-i\omega t} \tag{2.32}$$

For ideal temporal coupling between the source and the acoustic wave, ω must correspond to one of the resonant frequencies of the chamber. Since the time dependence of the velocity potential follows that of the source, $\phi(r,t)$ may be expressed as,

$$\phi(r,t) = f(r) e^{-i\omega t} \tag{2.33}$$

Substituting (2.32) and (2.33) into the wave equation (2.30) eliminates the time dependence.

$$\nabla^2 f + k^2 f = \frac{\gamma - 1}{\rho_o c^2} W \qquad (2.34)$$

where

$$k^2 = \frac{\omega^2}{c^2} \left(1 + \frac{i}{q} \right)$$

For radial symmetry in cylindrical coordinates the Laplacian operator is:

$$\nabla^2 = \frac{1}{r} \frac{d}{dr} \left(r \frac{d}{dr} \right) \qquad (2.35)$$

A solution for f(r) is assumed to be a series of zeroth order Bessel functions corresponding to the purely radial modes.

$$f(r) = \sum_n B_n J_o (\alpha_{o,n} r) \qquad (2.36)$$

Application of the first boundary condition (2.31) defines the radial wavenumber $\alpha_{o,n}$ in terms of the zeroes, $x_{o,n}$, of

$\frac{dJ_o(x)}{dx} = -J_1(x) = 0$, where $\alpha_{o,n} R = x_{o,n}$. The resonant frequencies are then given by,

$$\omega_n = \alpha_{o,n} c \qquad (2.37)$$

A complete solution is available after the evaluation of B_n. Combination of (2.35), (2.36) with (2.34) and simplification yields,

$$B_n \frac{\omega^2}{qc^2} \; i \, J_o \, (\alpha_{o,n} r) = \frac{\gamma - 1}{\rho_o c^2} W(r) \tag{2.38}$$

B_n can be determined by exploiting the orthogonality of the Bessel functions.

$$\int_o^R J_o(\alpha_{o,n} r) \, J_o(\alpha_{o,m} r) r dr = \begin{matrix} 0 & n \neq m \\ \tfrac{1}{2}R^2 \, J_o{}^2(\alpha_{o,n} R) & n = m \end{matrix} \tag{2.39}$$

making the appropriate integration of (2.38) yield,

$$B_n = - \frac{2(\gamma - 1) \; q \; i}{\omega^2 R^2 J_o{}^2 (\alpha_{o,n} R) \rho_o} \int_o^R W(r) \; J_o(\alpha_{o,n} r) r dr \tag{2.40}$$

Thus, once the energy distribution W(r) is known, the velocity potential can be uniquely determined for each resonant mode. All that is left is to apply (2.27) to obtain the perturbation pressure response.

$$p' \; (r,t) = (i - \frac{1}{q}) \; B_n \; \omega \rho_o J_o(\alpha_{o,n} r) e^{=i\omega t} \tag{2.41}$$

A second method for coupling between the source and the chamber involves longitudinal modes. In this case the source is placed at one end so that the entire cross-section of the chamber is illuminated. Plane waves would then propagate along this axis of symmetry.

We again seek solutions to (2.29) where the Laplacian operator for this case is

$$\nabla^2 = \frac{d^2}{dz^2} \tag{2.42}$$

The forcing function, in its general form, takes on both z and t dependence which for a purely modulated source is

$$Q(z,t) = Z(z)e^{-i\omega t} \tag{2.43}$$

In a similar manner the velocity potential can be taken as,

$$Q(z,t) = g(z)e^{-i\omega t} \tag{2.44}$$

Substitution of (2.43) and (2.44) into the wave equation and cancelling out the time factor yields,

$$\frac{d\ g}{dz^2} + \left(\frac{\omega^2}{c^2} + \frac{\omega^2}{c^2 q}\ i\right)g = \frac{\gamma-1}{\rho_o c^2}\ Z \tag{2.45}$$

A solution for g is assumed to be

$$g(z) = \sum_n A_n \cos k_n\ z \tag{2.46}$$

Application of the second boundary condition in (2.31) defines the allowed wavenumbers.

$$k_n = \frac{n\pi}{L} \quad n = 1,\ 2,\ 3\ .\ .\ . \tag{2.47}$$

The allowed frequencies in terms of the k_n are $\omega_n = ck_n$. Substitution of the solution (2.46) into (2.45) provides the result,

$$A_n \frac{\omega^2}{c^2 q}\ i \cos k_n z = \frac{\gamma-1}{\rho_o c^2}\ Z \tag{2.48}$$

To solve for the A_n, multiply both sides of (2.48) by cos $(k_m z)$ and integrate over the length of the chamber from z=0 to z=L. Because of the orthgonality of cos $k_n z$, the integral will be zero unless m=n. The constants are thus given by,

$$A_n = - \frac{2(\gamma-1)q\ i}{\omega^2 L} \int_o^L Z(z)\ \cos(k_n z) dz \qquad (2.49)$$

The solution is completely specified once the distribution of energy is known. The perturbation pressure is again given by (2.41) with A_n replacing B_n and cos $k_n z$ replacing J_o $(\alpha_{o,n} r)$ in this case.

The distribution of the acoustic signal is now predictable once the damping properties of the system and the energy distribution of the source are known for the mode of interest.

2.3 Energy Dissipation Mechanisms

The term K_o was introduced in the previous discussion to account for the acoustic damping in the system. Various mechanisms which contribute to the damping are examined, leading to a total damping for each resonant system.

In order to more easily compare the individual loss mechanisms, H is introduced and defined as the ratio of the energy loss per cycle to the total standing wave energy. The quality factor or "q" of the resonant peak is defined as $\frac{2\pi}{H}$. To a good approximation the various losses are not coupled and the total H will just be the sum of the individual H values.

Thermal losses occur because of non-equilibrium conditions that exist between neighboring regions of compression and rarefaction. Viscous losses are due to frictional dissipation of compressional motion. An expression for the attenuation factor for these mechanisms Morse and Ingard (1968, p. 277) is,

$$A = \tfrac{1}{2}(\eta + \frac{4}{3}\mu)\frac{k^2}{\rho_o c}\left(1 + \frac{\chi}{c_p}\,\frac{\gamma-1}{\eta+\frac{4}{3}\mu}\right) \tag{2.50}$$

where the wavenumber $k = \frac{\omega}{c}$ and μ and η are the first and second coefficients of viscosity. At a frequency $\frac{\omega}{2\pi} = 500\text{Hz}$ the value of the attenuation $A \simeq 1 \times 10^{-7}\ \text{cm}^{-1}$. Over a distance of 50 cm corresponding to the distance between two reflections of the wave, the fractional energy loss is roughly 5 x 10^{-6} which will be shown to be negligible compared to other losses.

Another source of energy loss in free space is the effect of vibrational relaxation. On gaining equilibrium due to the heating that takes place locally during compression, the individual molecules are forced into higher vibrational states. After compression has passed some of the energy remains in these states. Through inter-molecular collisions, this energy is transferred to other parts of the wave in a characteristic vibrational relaxation time. Kamm (1973) indicates that at a frequency of 4000 Hz., the H value is an order of magnitude less than losses due to the interaction of the wave with the chamber walls. At a frequency of 300 Hz. the relaxation losses would be even less significant.

In a closed chamber, losses are due to the interactions of the acoustic wave with the chamber walls. Viscous and thermal losses at the wall are generally the dominant effect in the total damping of the system. Thermal losses result from the non-adiabatic interaction of the acoustic wave with the walls. Viscous losses occur at boundaries where there is a velocity shear, i.e., where the wave motion has a tangential component at a boundary. The following analysis will assume perfect cylindrical geometry. In fact, certain irregularities such as the presence of the microphone may add substantially to the total damping.

We will consider the radial modes first. For purely radial motion only the end plates would contribute to viscous losses. It is interesting to note that for radial motion in the elliptical cavity, viscous losses would also occur at the radial boundary since in general the wave is incident at an angle other than 90^o to the boundary. This may be an important point in comparing these two geometries. Thermal losses occur at all boundaries. Expressions are provided (Morse and Ingard, 1968, pp. 291-292) for the power losses per unit area corresponding to thermal and viscous boundary losses respectively.

$$L_{bh} = \frac{\gamma-1}{4\rho_o c^2} \omega d_h \; | p'_{max} |^2 \qquad (2.51)$$

where d_h is the thermal boundary layer thickness given by,

$$d_h = \left(\frac{2\chi}{\rho_o \omega c_p} \right)^{\frac{1}{2}} \qquad (2.52)$$

and $| p'_{max} |$ is the magnitude of the time independent part of the perturbation pressure.

$$L_{bv} = \left(\frac{k_t c}{\omega}\right)^2 \left(\frac{\omega}{4\rho_o c^2}\right) d_v \; | p'_{max} |^2 \qquad (2.53)$$

where k_t is the tangential wave number at the boundary and d_v is the viscous boundary layer thickness defined by,

$$d_v = \left(\frac{2\mu}{\rho_o \omega}\right)^{1/2} \qquad (2.54)$$

μ being the viscosity of the medium. From (2.41) it is evident that,

$$p'_{max} = P_{max} J_o \, (\alpha_{o,n} r) \qquad (2.55)$$

In order to obtain the total power loss from the two mechanisms, it is necessary to integrate the losses per unit area over the appropriate surface areas.

$$\text{Thermal Loss } P_{bh} = \int_o^L \int_o^{2\pi} \frac{\gamma-1}{4\rho_o c^2} \, \omega d_h \, p^2_{max} J_o^{\,2} (\alpha_{o,n} R) \; R d\theta \, dz$$

$$+ 2 \int_o^{2\pi} \int_o^R \frac{\gamma-1}{4\rho_o c^2} \, \omega d_h \, p^2_{max} \, J_o^{\,2} \, (\alpha_{o,n} r) \; r dr d\theta \qquad (2.56)$$

This results in the final expression,

$$P_{bh} = \frac{\gamma-1}{2\rho_o c^2} \, \omega d_h \, p^2_{max} J^2 (\alpha_{o,n} R) \; \pi R^2 (1+\frac{L}{R}) \qquad (2.57)$$

$$\text{Viscous Loss } \; P_{bv} = 2 \int_o^{2\pi} \int_o^R \left(\frac{k_t c}{\omega}\right)^2 \left(\frac{\omega}{4\rho_o c^2}\right) d_v \, p^2_{max} \, J_o^{\,2}$$

$$(\alpha_{o,n} r) \; r dr d\theta \qquad (2.58)$$

For the case of the radial waves, the tangential wavenumber, k_t, at the ends is just the radial wavenumber $\alpha_{o,n}$. This results in,

$$P_{bv} = \frac{\omega}{2\rho_o c^2} \underset{\downarrow}{dv}\, p^2{}_{max}\, J_o{}^2\, (\alpha_{o,n}R)\,\pi R^2 \qquad (2.59)$$

The total power loss, P_b is the sum of the thermal and viscous losses. We are interested in the total energy loss per cycle, E_b, which is equal to $\frac{P_b}{f}$ where $2\pi f = \omega$.

$$E_b = \frac{\pi^2 R^2}{\rho_o c^2}\, p^2{}_{max}\, J_o{}^2(\alpha_{o,n}R)\, [\underset{\downarrow}{dv} + (\gamma-1)\underset{\downarrow}{dh}(1+\frac{L}{R})] \qquad (2.60)$$

We now need the total standing wave energy E_t. The acoustic wave energy density is given by [4] p. 258.

$$w = \frac{1}{2}\, \frac{|p'_{max}|^2}{\rho_o c^2} \qquad (2.61)$$

E_t is obtained by integrating w over the entire chamber volume, the result being,

$$E_t = \frac{\pi R^2 L}{2\rho_o c^2}\, p^2{}_{max}\, J_o{}^2(\alpha_{o,n}R) \qquad (2.62)$$

The damping parameter H is just the ratio of E_b to E_t.

$$H = \frac{2\pi}{L}\, [\underset{\downarrow}{dv} + (\gamma-1)\underset{\downarrow}{dh}\, (1 + \frac{L}{R})] \qquad (2.63)$$

Substituting in for d_v and d_h and noting that ω can be expressed in terms of R, we obtain the desired expression for H.

$$H = (\frac{8\pi^2\mu}{\rho_o c x_{o,n}})^{\frac{1}{2}}\, (\frac{R^{\frac{1}{2}}}{L} + \frac{\gamma-1}{(\mu c_p/\chi)^{\frac{1}{2}}}\, (\frac{R^{\frac{1}{2}}}{L}\quad \frac{1}{R^{\frac{1}{2}}}) \qquad (2.64)$$

It remains to show the relationship of H to the damping factor q used in the wave equation. To do this we wish to determine the response of the system once the energy source has been removed. The equation for a purely damped wave is,

$$\frac{1}{c^2} \quad \frac{d^2\phi}{dt^2} = \nabla^2\phi + \frac{\omega}{c^2 q} \quad \frac{\partial\phi}{\partial t} = 0 \tag{2.65}$$

Since H is the fractional energy dissipation per cycle and the energy of the acoustic wave is proportional to the pressure squared or the velocity potential squared, we assume a solution of the form,

$$\phi(r,t) = A_1 \; J_o(\alpha_{o,n} r) e^{\left(-\frac{H}{2} + 2\pi i\right) ft} \tag{2.66}$$

Substituting the solution into the damped wave equation yields,

$$\left(- \frac{Hf}{2} + 2\pi i f\right)^2 + \omega^2 + \frac{\omega f H}{2q} + \frac{\omega^2}{q} = 0 \tag{2.67}$$

Noting that $\omega = 2\pi f$ and neglecting terms of second order in H and $\frac{1}{q}$ we obtain the desired result,

$$q = \frac{2\pi}{H} \tag{2.68}$$

Thus the damping factor used to obtain the pressure distribution is identically the quality factor of the resonance.

In order to examine how q varies as a function of the chamber parameters L and R, for radial modes, we will assume that the damping is due only to thermal and viscous losses at the boundaries. From (2.64) and (2.68) we can write

$$\frac{1}{q} \propto \frac{R^{\frac{1}{2}}}{L} + c_2 \left(\frac{R^{\frac{1}{2}}}{L} + \frac{1}{R^{\frac{1}{2}}}\right) \tag{2.69}$$

where

$$c_2 = \frac{\gamma-1}{(\mu c_p/\chi)^{\frac{1}{2}}}$$

Over a temperature range from -40°C to +30°C the value of c_2 is very nearly constant and equal to 0.47. For simplicity of analysis we take $c_2 = \frac{1}{2}$.

$$\frac{1}{q} \propto \frac{3R^{\frac{1}{2}}}{2L} + \frac{1}{2R^{\frac{1}{2}}} \tag{2.70}$$

$$q \propto \frac{2LR^{\frac{1}{2}}}{3R+L} \tag{2.71}$$

The energy losses from the longitudinal modes can be found in a similar manner. Noting that in this case viscous losses take place along the side wall, (2.51) and (2.52) can be integrated over the appropriate areas where,

$$p'_{max} = p_{max} \cos k_n z \tag{2.72}$$

The results are,

$$\text{Thermal loss } P_{bh} = \frac{\pi R^2 \ (\gamma-1)\omega d_h \ P^2_{max}}{2\rho_o c^2}[1 + \frac{L}{R}] \tag{2.73}$$

$$\text{Viscous loss } P_{bv} = \frac{\pi R^2 L \omega d_v \ p^2_{max}}{4\rho_o c^2} \tag{2.74}$$

The tangential wave number k_t used in the viscous loss is just the longitudinal wavenumber k_n. The total power loss, P_b is the sum of the thermal and viscous loss. The total energy loss per cycle then is P_b/f where $2\pi f = \omega$.

$$E_b = \frac{\pi^2 R^2 p^2_{max}}{\rho_o c^2} [\ d_v \frac{L}{2R} + (\gamma-1) \ d_h \ (1 + \frac{L}{2R}) \ ] \tag{2.75}$$

The total acoustic energy in the system is again determined by integrating the energy density (2.61) using (2.72) over the entire chamber volume.

$$E_t = \frac{\pi R^2 L \ p^2_{max}}{4\rho_o c^2} \tag{2.76}$$

The damping parameter H is the ratio of E_b to E_t

$$H = \frac{4\pi}{L} [\ d_v \ \frac{L}{2R} + (\gamma-1) \ d_h(1 + \frac{L}{2R}) \ ] \tag{2.77}$$

Substituting in for d_n and d_v and expressing ω in terms of L leads to the final result.

$$H = \left(\frac{16\pi\mu}{\rho_o cn}\right)^{\frac{1}{2}} \left[\frac{L^{\frac{1}{2}}}{2R} + \frac{(\gamma-1)}{(\mu c_p/\chi)^{\frac{1}{2}}} \left(\frac{1}{L^{\frac{1}{2}}} + \frac{L^{\frac{1}{2}}}{2R} \right) \right] \tag{2.78}$$

In terms of the chamber parameters,

$$\frac{1}{q} \propto H \propto \frac{L^{\frac{1}{2}}}{2R} + c_2 \left(\frac{1}{L^{\frac{1}{2}}} + \frac{L^{\frac{1}{2}}}{2R} \right) \tag{2.79}$$

where c_2 is the same value as used in the radial mode case.

$$\frac{1}{q} \propto \frac{1}{2L^{\frac{1}{2}}} + \frac{3L^{\frac{1}{2}}}{4R} \tag{2.80}$$

$$q \propto \frac{4RL^{\frac{1}{2}}}{2R+3L} \tag{2.81}$$

The dependence of the q values on the chamber parameters are used with (2.41) for each mode case, once the energy distribution is known, to determine how the pressure depends on the chamber parameters.

2.4 Optical Coupling

Consideration is given now to how the spatial distribution of the optical source relates to the pressure distribution. As has been shown in section 2.1, equation (2.2) gives the acoustic source. I_o is the intensity of the optical source which is assumed to be parallel with a total power P_o. We want to determine how the pressure depends on P_o and finally on the chamber parameters.

We first consider the radial modes. The optical source is incident along the axis of symmetry of the chamber. We take the intensity to be constant across the beam diameter so that in (2.32) W(r) is given by,

$$W(r) = \begin{cases} \dfrac{\alpha I_o}{2} & 0 \leq r \leq b \\ 0 & r > b \end{cases} \tag{2.82}$$

Where b is the radius of the beam cross section.

We can now determine the $B_{n's}$ from (2.40). However since we are interested only in the first order mode, only B_1 need be considered. Note also that $I_o = \dfrac{P_o}{\pi b^2}$.

In terms of the variable parameters (q, R, P_o, b)

$$B_1 \propto \frac{qP_o}{\pi b^2} \int_0^b J_o(\alpha_{o,n} r) rdr \tag{2.83}$$

After simplifying the result of the integration noting that

$$\alpha_{o,1} = \frac{x_{o,1}}{R},$$

$$B_1 \propto \frac{qP_o}{\frac{x_{o,1}b}{R}} J_1\left(\frac{x_{o,1}b}{R}\right) \qquad (2.84)$$

From the series representation of J_1 for $b<<R$

$$J_1\left(\frac{x_{o,1}b}{R}\right) = \frac{x_{o,1}b}{2R}, \text{ therefore,}$$

$$B_1 \propto \frac{qP_o}{2} \qquad (2.85)$$

This last assumption of $b<<R$ maximizes B_1 which ultimately helps to maximize p'. It is evident from (2.41) that for $q^2>>1$,

$$p' \propto B_1\omega \propto \frac{qP_o}{2R} \qquad (2.86)$$

Substituting in the dependence of q from (2.71) yields the result,

$$p' \propto \frac{LP_o}{(3R+L)R^{\frac{1}{2}}} \qquad (2.87)$$

Since we are constrained in our use of the modulation frequency, R is a fixed quantity. Equation (2.87) is thus maximized for $L>>R$ leading to the final result,

$$p' \propto \frac{P_o}{R^{1/2}} \tag{2.88}$$

Next we consider the case of longitudinal modes. In this case the optical source is incident from the side and is confined to a small volume at one end. The beam has a rectangular cross section of width d and height 2R so that the beam fills up the cross sectional area of the chamber. The source function z is given by,

$$Z(z) = \frac{\alpha I_o}{2} \qquad 0 \leq z \leq d \tag{2.89}$$

$$= 0 \qquad z > d$$

In terms of the power in the beam $I_o = \frac{P_o}{2Rd}$. Again we consider only the first order mode so that $\omega = \frac{\pi c}{L}$. Substituting in for Z(z) in (2.49) results in

$$A_1 \propto \frac{qP_o}{dR\omega} \int_o^d \cos\left(\frac{\pi z}{L}\right) dz \tag{2.90}$$

After simplifying the result,

$$A \propto \frac{qP_o \sin\frac{\pi z}{L}}{R\omega \; \frac{\pi d}{L}} \tag{2.91}$$

For $d \ll L$, $\sin \frac{\pi d}{L} \doteq \frac{\pi d}{L}$, leaving

$$A_1 \propto \frac{qP_o}{\omega R} \qquad (2.92)$$

Again for $q^2 \gg 1$ the pressure is given by

$$p' \propto \frac{qP_o}{R} \qquad (2.92)$$

Substituting in for q from (2.81) yields

$$p' \propto \frac{4L^{\frac{1}{2}}P_o}{2R+3L} \qquad (2.93)$$

In this case the modulation frequency fixes L. The maximum value of p' occurs for $R \ll L$.

$$p' \propto \frac{4P_o}{3L^{\frac{1}{2}}} \qquad (2.94)$$

If we now include any proportionality constants in (2.87) and (2.94) that are not the same in both equations, we can ultimately compare the magnitude of the pressure of each mode. Thus (2.88) becomes

$$p' \propto \frac{1}{(\pi x_{o,1})^{\frac{1}{2}}} \; \frac{P_o}{R^{\frac{1}{2}}} \qquad (2.95)$$

and (2.94) becomes

$$p' \propto \left(\frac{1}{8\pi^2} \right)^{\frac{1}{2}} \frac{4P_o}{3L^{\frac{1}{2}}} \qquad (2.96)$$

CHAPTER 3

OPTIMIZATION OF CHAMBER DESIGN

3.1 Experimental Confirmation of Chamber Resonance and Damping Properties

In this section we make use of the various resonant situations discussed in the previous chapter to determine how well the resonance and damping properties can be predicted by the theory.

We first consider the radial modes. For the lowest order resonant frequency $f_o \simeq 300$ Hz, eq. (2.37) indicates that $R \simeq 70$ cm. Since this makes for a very large chamber, a more convenient size was chosen for testing purposes. The cylindrical chamber thus used had a radius $R = 5.08$ cm and length $L = 15.24$ cm. At a temperature of 20°C the lowest resonant frequency given by eq. (2.37) is $f_o = 4110$ Hz. In order to make a closer comparison with the cylindrical chamber, the elliptical chamber was designed with a semi-major axis of 5.08 cm, a length of 16.70 cm and an eccentricity of 0.5. This eccentricity places the focal lines midway between the center and the wall.

It was first necessary to have a method of exciting the modes, which is similar to the ultimate use of an optical source. The method chosen is the thermophone technique (see Arnold and Crandall, 1917, and Wente, 1928, for a more detailed description). The technique involves driving a thin strip of metal foil with an alternating current. Periodic heating and cooling takes place in the foil, the heat being transferred to the surrounding air thus generating a pressure wave. It turns out that for pure alternating current, heating takes place during each half cycle and the frequency of the applied source must be one-half that of the desired resonance. The particular foil used was a nickel foil of thickness 1.9 microns. Even though the foil is flat, if its size is kept small with respect to the radial dimension of the chamber, it approximates a radial source. For the elliptical case it was placed along one of the focal lines. The same strip was used in testing both chambers.

The pressure wave is detected by a TE Electret condenser microphone model 533b developed by Thermo-Electron Corporation. The microphone has a flat response over a frequency range of 50-16,000 Hz with a sensitivity of 1 m volt per μbar. The miniature size (.711 cm x .711 cm x .406 cm) is an advantage in minimizing effects due to the presence of the microphone. In order to accurately measure the signal in the presence of noise, a P. A. R. model HR-8 lock-in amplifier was used.

Using this system the lowest order radial mode of the cylindrical chamber was measured to be $f_o = 4175$ Hz. Comparison with the theoretical value shows agreement within 2%.

Since the resonant frequency is temperature dependent through the speed of sound, the difference is probably due to inexact knowledge of the temperature inside the chamber.

The q of the resonance can be determined from measurement by

$$q = \frac{f_o}{f_2 - f_1} \tag{3.1}$$

Where f_2 and f_1 are the frequencies on either side of the peak, f_o, where the acoustic power falls to one-half of the value at the peak. Since the acoustic power varies as the square of the pressure amplitude, the half power frequencies occur where the pressure amplitude falls to 0.707 the value at the peak.

This equation, (3.1), is based on the resonance of a mechanical vibrating spring model having a damping factor associated with it and being driven in one of the resonant modes. The complete result of the model giving the ratio of the signal amplitude at any frequency to that at the peak for the application to a high q bank pass electronic filter is (Graeme, Tobey, and Huelsman, 1971, p. 286).

$$H(S) = \frac{H_o \frac{1}{q} \omega_o S}{S^2 + \frac{1}{q} \omega_o S + \omega_o^2} \tag{3.2}$$

where $S = i\omega$.

$$\left| \frac{H(S)}{H_o} \right| = \frac{A}{A_o} = \frac{\frac{1}{8} \quad \frac{f}{f_o}}{\left[\; (1-(\frac{f}{f_o})^2 + (\frac{1}{q} \; \frac{f}{f_o} \;)^2 \right]^{\frac{1}{2}}} \tag{3.3}$$

The procedure then was to determine peak signal and peak frequency by varying the frequency of the signal source until a maximum signal was obtained. The frequency was measured by a Hewlett-Packard model 5300 A frequency meter which can be read to ±0.1 Hz. The signal source frequency was then varied until the half power points were reached on each side of the peak. Using (3.1) the experimental value of q was found to be $q_{ex.} = 600 \pm 60$. The uncertainty is due to uncertainties in the signal values as well as the frequencies. Using (2.64) with R=5.08 cm and L = 15.24 cm, the theoretical value of q is found to be $q_{th} = 1408$. Evidently mechanisms other than thermal and viscous losses at walls are important or the particular model used is incorrect.

Measurements were also made on the strongest elliptical resonance in the elliptical chamber. The resonant frequency was determined to be $f_o = 7566$ Hz. The q determined in the same way as above from (3.1) is $q_{ex.} = 630 \pm 60$.

For the case of the longitudinal modes, it was convenient to design a chamber to more closely fit the specifications of Chapter 2. The length L=55 cm and the radius R=2.5 cm. From (2.47) the lowest order resonant frequency at 20^{o}C is given by $F_o = 312$ Hz.

A different method was used to excite the longitudinal modes. A speaker was placed external to the chamber, oriented so that its face was normal to the long axis of the chamber. In this way the energy is coupled into the chamber through the end wall. Thus the source is confined to a small volume at one end which would also be the case using an optical source.

The lowest order frequency was measured to be f_o = 315 Hz. Comparison with the theoretical value of 312 Hz indicates agreement within 1%. Using (3.1) as before the experimental q was determined to be $q_{ex.} = 61 \pm 2$. Use of (2.78) with the size parameters given above gives the theoretical q to be $q_{th} = 172$. Again the agreement between experimental and theoretical values is not good. Figure 2 shows a curve of (3.3) with a q = 61 plotted with the experimental points of the resonance profile. The agreement is very good near the peak and begins to deviate slightly further away from the peak on the right hand side. Figure 2 thus indicates that the model used to determine the experimental q values is not the reason for the lack of agreement with the theory.

The measured q value in each case seems to be predictable only in a qualitative sense. However the degree of agreement is similar for the longitudinal and radial mode, in spite of differences in chamber sizes. Thus the use of the results of section 2.3 in predicting the pressure response as a function of the chamber parameters seems to be reasonable.

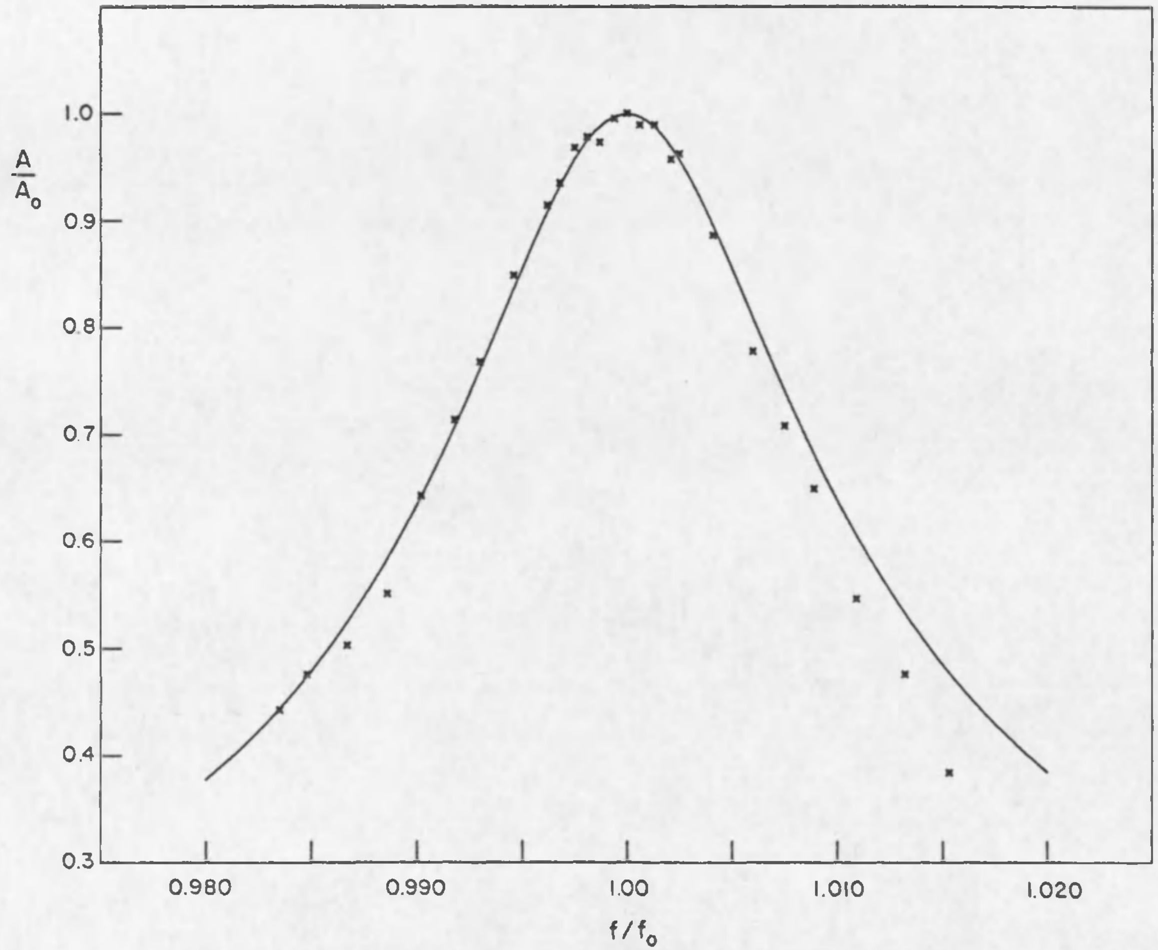

Fig. 2 Longitudinal Resonance Profile

3.2 Comparison of Chambers

In this section we intend to use the results of the previous sections to finally determine which resonant mode, and hence which chamber design, allows for the optimum response of the entire system.

Comparison of the cylindrical with the elliptical radial resonances indicates that the values of the q are quite similar. In addition, the measured output signal for the same input in both cases was very nearly the same. There is no overriding reason for choosing to use the elliptical geometry rather than the cylindrical. Due to the comparative case in which the cylindrical geometry can be theoretically predicted, it would be preferred in this respect. We originally thought that, because of the focussing properties of the ellipse, the measured signal would be stronger; however, this is not evident. There are no readily obvious reasons for this occurrence.

We assume, as concluded in section (3.1), that the q dependence on the chamber parameters developed in Chapter 2 is valid. The maximum pressure response, under the assumption of a small geometrical size of the optical source compared with the chamber size, is given by (2.95) and (2.96) and reproduced here.

Longitudinal mode $$p' \propto \left(\frac{1}{8\pi^2} \right)^{\frac{1}{2}} \frac{4P_o}{3L^{\frac{1}{2}}} \qquad (3.4)$$

Radial mode $$p' \propto \left(\frac{1}{\pi x_{o,1}}\right)^{\frac{1}{2}} \frac{P_o}{R^{\frac{1}{2}}} \tag{3.5}$$

where $x_{o,1} = 3.832$.

In both cases it was also taken that L>>R. The chamber using longitudinal modes has R=2.5 cm L = 55 cm at a frequency of 312 Hz. The radial mode chamber would require R = 67 cm for a similar resonant frequency. Thus for L>>R a length of at least 670 cm would be required. Equations (3.4) and (3.5) indicate that the pressure response is very similar, within a factor of 2. There are no compelling reasons from a purely signal strength point of view for choosing one mode over the other.

The longitudinal chamber has a much more convenient size. The radial chamber, being very large, would be difficult to build accurately. For most construction materials it would be extremely heavy making its usefulness in field experiments limited.

A much more compelling reason for choosing to use the longitudinal chamber comes from an examination of the q's. The actual q of the longitudinal chamber was given in section (3.1) as 61. Substituting the size parameters for the radial chamber into (2.64) yields a theoretical q of about 8000. A more realistic q in an actual chamber might be 2000. Figure 2 shows that as the signal frequency moves off resonance the amplitude decreases. In the longitudinal case for amplitude deviations of ± 2%, figure 2 indicates that for f_o = 312 Hz the frequency deviation is ± 0.5 Hz. Since the q of the radial chamber is a factor of 30 greater, then the allowed frequency deviation at the 2% level is more like ± .02 Hz. One cause of the signal frequency drifting away from resonance would be drift in the chopping system which modulates the optical beam. A chopping system stable to ± 0.5 Hz is not difficult to achieve, but trying to correct for instability of ± .02 Hz, though it may be possible, would add to the complexity. The resonant frequency itself varies with temperature through the speed of sound.

$$f_o = T^{\frac{1}{2}} \tag{3.6}$$

The ± 0.5 Hz criteria corresponds to a temperature stability of ± 0.9°K at 20°C. For the radial chamber the ± 0.02 Hz criteria corresponds to temperature fluctuations of ± 0.03°K at 20°C.

It is obvious that, in addition to not providing any greater signal response, the radial chamber does place very stringent stability requirements on the system. We conclude that, in keeping with desire to have the system as simple and flexible as possible, the longitudinal modes should be used.

There is no compelling reason for choosing a modulation frequency of 312 Hz. However we desire to have as large a frequency as possible within the constraints in section 2.1

so as to have as large a pressure signal as possible. Given the frequency of 312 Hz, this fixes the length to be L = 55 cm. R is chosen to be 2.5 cm in line with L>>R to maximize the pressure response. The width, d, of the optical source must be small so that $\sin\left(\frac{\pi d}{L}\right) = \left(\frac{\pi d}{L}\right)$. For agreement within 1% must be no greater than 4.4 cm.

CHAPTER 4

CONCLUDING REMARKS

The study presented here is only a part of a broader project to design a practical system for measuring aerosol absorption. Using the longitudinal mode with an optical source distributed as given in (2.89), a measurement of the pressure response, p', coupled with the use of (2.41) for longitudinal modes, is sufficient to determine α. The value of q used should be the experimentally determined value.

One area of further concern is to determine the power needed from the optical source. Useful measurements require that α be measurable to 10^{-7}-10^{-8} cm^{-1}. The limiting factor for signal measurement is the noise level in the band width of the look-in amplifier. Therefore study must be done on the various noise factors contributing to the problem in order to minimize the required optical power as much as possible. It is also noted that the power P_o, used in this study is the power delivered to the particles in the chamber.

It is also necessary to determine the extent to which the analysis in section (2.1) is valid. For this a known physical properties Equation (2.17) can then be used to calculate α and comparisons made with measured values. Samples should be used at a variety of particle sizes.

Other aspects of the system such as getting the samples in and out of the chamber and coupling the optical source into the source region which could include a multiple pass arrangement to effectively increase the power of the source should also be considered.

In all these considerations where possible we must attempt to keep the system as uncomplicated as possible since an overly complex system would tend to be too limited in its usefulness.

LIST OF REFERENCES

Arnold, H. D., and I. B. Crandall. "The Thermophone as a Precision Source of Sound," Physical Review, 2nd Series, Vol. 10, No. 1, 1917, pp. 22-38.

Atwater, Marshall S. "Radiative Effects of Pollutants in the Atmospheric Boundary Layer," J. of Atmospheric Sciences, Vol. 24, No. 11, 1971, pp. 1367-1373.

Compton, Dale L. Radiatively Driven Acoustic Waves In a Cylindrical Tube--Theory and Experiment at Resonance, Department of Aeronautics and Astronautics Stanford University, SUDDAR No. 385, August 1969.

Fuchs, N. A., and A. G. Sutugin. Highly Dispersed Aerosols, Ann Arbor, Michigan: Ann Arbor Science Publishers, 1970.

Graeme, Jerald D., Gene E. Tobey, and Lawrence P. Huelsman. Operational Amplifiers--Design and Application, New York: McGraw-Hill, 1971.

Kamm, Roger D. An Acoustic Amplifier For the Detection of Atmospheric Pollutants, M.S. Thesis, Department of Mechanical Engineering, M.I.T., 1973.

Kruezer, L. B. "Ultralow Gas Concentration Infrared Absorption Spectroscopy," J. of Applied Physics, Vol. 42, No. 7, 1971, pp. 2934-2943.

Morse, P. M., and K. Ingard. Theoretical Acoustics, New York: McGraw-Hill, 1968.

Rayleigh, Lord. Theory of Sound, 2nd Edition, New York: Dover Publications, 1945.

Wente, Edward C. "The Thermophone," Physical Review, 2nd Series, Vol. 19, No. 4, 1928, pp. 333-345.